Biochimica et Biophysica Acta 1838 (2014) 940–949

Contents lists available at ScienceDirect

Biochimica et Biophysica Acta

journal homepage: www.elsevier.com/locate/bbamem

Dynamical structure of the short multifunctional peptide BP100 in membranes

Parvesh Wadhwani [a], Erik Strandberg [a], Jonas van den Berg [b], Christian Mink [b], Jochen Bürck [a], Raffaele A.M. Ciriello [b], Anne S. Ulrich [a,b,*]

[a] Karlsruhe Institute for Technology (KIT), Institute for Biological Interfaces (IBG-2), POB 3640, 76021 Karlsruhe, Germany
[b] KIT, Institute of Organic Chemistry and CFN, Fritz-Haber-Weg 6, 76131 Karlsruhe, Germany

ARTICLE INFO

Article history:
Received 25 July 2013
Received in revised form 25 October 2013
Accepted 1 November 2013
Available online 9 November 2013

Keywords:
Antimicrobial peptide BP100
Amphipathic α-helix
Solid state ^{15}N NMR and ^{19}F NMR
Dynamical NMR data analysis
Oriented circular dichroism
Peptide orientation and dynamics

ABSTRACT

BP100 is a multifunctional membrane-active peptide of only 11 amino acids, with a high antimicrobial activity, an efficient cell-penetrating ability, and low hemolytic side-effects. It forms an amphiphilic α-helix, similar to other antimicrobial peptides like magainin. However, BP100 is very short and thus unlikely to form membrane-spanning pores as proposed for longer peptides as a mechanism of action. We thus studied the conformation, membrane alignment and dynamical behavior of BP100 in lipid bilayers (DMPC/DMPG), using oriented circular dichroism (OCD) and solid-state ^{19}F and ^{15}N NMR. According to OCD and ^{15}N NMR, the BP100 helix is oriented roughly parallel to the membrane surface, but these methods yield no information on the azimuthal alignment angle or the dynamics of the molecule. To address these questions, a systematic ^{19}F NMR analysis was performed, which was not straightforward for this short peptide. Only a limited number of positions could be ^{19}F-labeled, all of which are located on one face of the helix, which was found to lead to artifacts in the data analysis. It was nevertheless possible to reconcile the ^{19}F NMR data with the OCD and ^{15}N NMR data by using an advanced dynamical model, in which peptide mobility is described by fluctuating tilt and azimuthal angles with Gaussian distributions. ^{19}F NMR thus confirmed the regular α-helical conformation of BP100, revealed its azimuthal angle, and described its high mobility in the membrane. Furthermore, the very sensitive ^{19}F NMR experiments showed that the alignment of BP100 does not vary with peptide concentration over a peptide-to-lipid molar ratio from 1:10 to 1:3000.

1. Introduction

Antimicrobial peptides (AMPs), also known as host defense peptides, are part of the innate immune system of most organisms [1–3]. They often form cationic amphiphilic structures that can kill bacteria by permeabilizing their membranes [4–6]. Much research has focused on the possibilities of developing new types of antibiotics from such peptides, as they tend to bear less risk of inducing bacterial resistance than conventional antibiotics [3,7]. Of special interest for pharmaceutical applications are short sequences that are easy and cost-efficient to synthesize. Many groups have systematically optimized naturally occurring AMPs, yielding amongst others the 11 amino acid peptide BP100 (KKLFKKILKYL-NH_2) [8]. Starting with hybrids of cecropin and melittin [9], the promising 11-mer Pep3 was developed [10]. Amongst 22 analogs of Pep3, the one with the highest antimicrobial activity was called BP76 [11]. In a further study, a library of 100 analogs of BP76 was produced and evaluated, amongst which BP100 was found to exhibit the best combination of high antimicrobial activity and low cytotoxicity and hemolysis [8]. Atomic force microscopy revealed that it destroys the cell envelope of *Escherichia coli* bacteria at a minimum inhibitory concentration of 3 μM [12]. This indicates that the cell membrane is the target of the peptide, and that membrane damage is the primary cause of the antibacterial effect. BP100 is a genuinely multifunctional peptide, because it is taken up, for example, into tobacco cells without causing leakage or being toxic [13], hence it is very useful also as a cell-penetrating peptide (CPP).

BP100 is predicted to form an amphiphilic helical structure in the presence of membranes, as confirmed here using circular dichroism; the helical wheel projection is shown in Fig. 1. It can be seen that one face of the helix consists of charged Lys residues, while all hydrophobic residues are on the opposite side. BP100 is only half as long as the well-known α-helical AMPs of the magainin family (magainin 2 with 23 amino acids [14]; PGLa [15], MSI-103 [16] and MSI-78 [17] with 21 residues each) or maculatin 1.1 with 21 residues [18]. The mode of action of these longer peptides is attributed to the formation of pores, in which the peptides assume a – possibly transient – membrane-spanning orientation to form an aqueous pore. The helix of BP100, however, is too short to span a typical biological membrane, as it has a length of 16.5 Å (1.5 Å per residue for an ideal α-helix) assuming that the peptide is completely helical. Therefore, it is unlikely to form transmembrane

* Corresponding author at: KIT, Institute of Organic Chemistry and CFN, Fritz-Haber-Weg 6, 76131 Karlsruhe, Germany. Tel.: +49 721 608 43222; fax: +49 721 608 44823.
E-mail address: anne.ulrich@kit.edu (A.S. Ulrich).

0005-2736/$ – see front matter © 2013 Elsevier B.V. All rights reserved.
http://dx.doi.org/10.1016/j.bbamem.2013.11.001

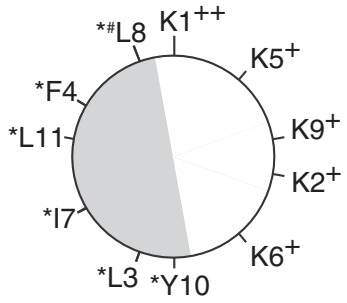

Peptide name	Sequence
BP100-WT	KKLFKKILKYL-NH_2
BP100-3L-Bpg	KK-CF_3-Bpg-FKKILKYL-NH_2
BP100-4F-Bpg	KKL-CF_3-Bpg-KKILKYL-NH_2
BP100-7I-Bpg	KKLFKK-CF_3-Bpg-LKYL-NH_2
BP100-8L-Bpg	KKLFKKI-CF_3-Bpg-KYL-NH_2
BP100-10Y-Bpg	KKLFKKILK-CF_3-Bpg-L-NH_2
BP100-11L-Bpg	KKLFKKILKY-CF_3-Bpg-NH_2
BP100-8L-^{15}N	KKLFKKI-^{15}N-Leu-KYL-NH_2
BP100-4F-Bpg-8L-^{15}N	KKL-CF_3-Bpg-KKI-^{15}N-Leu-KYL-NH_2
BP100-7I-Bpg-8L-^{15}N	KKLFKK-CF_3-Bpg-^{15}N-Leu-KYL-NH_2

Fig. 1. Helical wheel projection of BP100. The hydrophobic sector is shown in gray and the polar sector in white. Charged lysine residues and the N-terminus are marked with +, residues labeled with CF_3-Bpg are labeled with * and Leu8 which was also labeled with ^{15}N is labeled with #. The sequences of all synthesized peptides are also given.

pores, which raises the question as to which membrane bound orientation of BP100 is responsible for its mechanism of action.

A well-established method of investigating helical peptides in membranes is to determine the orientation of the helix in oriented lipid bilayers using solid-state NMR structure analysis [19–38]. The helix alignment is described by two angles: the tilt angle τ, defined as the angle between the long axis of the peptide and the membrane normal, and the azimuthal rotation angle ρ, which defines a rotation of the helix around its long axis. ^{15}N-labeling in the peptide backbone is routinely used to determine τ in straightforward 1-dimensional NMR experiments [27,30,39,40]. We have thus placed a ^{15}N-label into the backbone amide of a single residue of BP100 (Leu8), in order to estimate the tilt angle of this short helical peptide in membranes. ^{13}C NMR provides another, more sensitive approach to determine the orientation of peptides in membranes [32,35]. An even more sensitive method, based on the use of selective CF_3-labels, has been established by our group to obtain both τ and ρ with simple one-pulse ^{19}F NMR experiments [22–26,36,40–70]. In the present study, we have thus labeled BP100 with CF_3-*L*-Bpg [3-(trifluoromethyl)-*L*-bicyclopent-[1.1.1]-1-ylglycine] [68], replacing all hydrophobic residues, one at a time. This strategy has been successfully employed to characterize several longer AMPs, but has not been used on any short peptides such as BP100 or temporins. The selective substitution of each hydrophobic residue in BP100 by CF_3-*L*-Bpg is routinely feasible, but one should bear in mind that the ^{19}F NMR data analysis will only yield meaningful results if a high degree of secondary structure can be evidenced by CD, as demonstrated below. Membrane-bound BP100 indeed shows an unusually high helicity for an 11-mer peptide, which makes it a perfect candidate to examine the advantages and limitations of solid-state ^{19}F NMR structure analysis for shorter peptides. Given the short length of BP100 and the presence of 5 charged Lys residues forming a large polar sector (see Fig. 1), we note that all remaining hydrophobic residues that are available for replacement with CF_3-*L*-Bpg lie on one face of the helix. This arrangement can be expected to make the NMR data analysis uncertain, as will be demonstrated below. To overcome this potential ambiguity and to additionally test the influence of CF_3-*L*-Bpg labeling on this short peptide, non-perturbing ^{15}N-labels were introduced not only in the wild type BP100 (free of CF_3-*L*-Bpg), but also in some ^{19}F-labeled analogs (see Fig. 1).

Traditionally, membrane-bound peptides have been described only in terms of τ and ρ, but recently whole-body motions have been introduced as additional parameters in the NMR data analysis [71–73]. For several long AMPs it has been shown that their motions do not influence the NMR analysis much [72,74], whereas for some transmembrane helices of similar length it was crucial to take dynamics into account [72,75,76]. Here, we analyze the importance of dynamics for BP100, given that this very short peptide is likely to undergo more extensive fluctuations in liquid-crystalline membranes than the longer AMPs studied before. We furthermore combine ^{19}F and ^{15}N NMR with oriented circular dichroism (OCD) [77], an independent qualitative method to obtain orientational information on membrane-embedded α-helical peptides [47,78–86]. By using all these techniques to measure the orientation of BP100 in the same kind of oriented DMPC/DMPG samples, which are supposed to mimic microbial membranes, we show that the use of several complementary methods is advisable to get reliable results. Especially for very short peptides like BP100, dynamical effects are found to be much more important than for longer ones such as PGLa or magainin 2, and special care must be taken to include this mobility in an appropriate way in the final description of the system.

2. Materials and methods

2.1. Materials

Fmoc-protected amino acids and coupling reagents used for peptide synthesis were purchased from Iris Biotech GmbH (Marktredwitz, Germany) or Novabiochem (Merck Chemicals Ltd., Nottingham, UK). The ^{19}F-labeled amino acid 3-(trifluoromethyl)-*L*-bicyclopent-[1.1.1]-1-ylglycine (CF_3-Bpg) was purchased from Enamine (Kiev, Ukraine). Solvents for synthesis and purification were purchased from Biosolve (Valkenswaard, The Netherlands) or Acros Organics (Geel, Belgium). UV-grade chloroform and methanol used for sample preparation were obtained from VWR International (Bruchsal, Germany). The lipids 1,2-dimyristoyl-*sn*-glycero-3-phosphatidylcholine (DMPC) and 1,2-dimyristoyl-*sn*-glycero-3-phosphatidylglycerol (DMPG) were purchased from Avanti Polar Lipids (Alabaster, AL) and used without further purification.

2.2. Peptide synthesis

BP100, with the sequence KKLFKKILKYL-NH_2, was synthesized with a single CF_3-*L*-Bpg at six different positions (Leu3, Phe4, Ile7, Leu8, Tyr10, or Leu11); with ^{15}N-labeled leucine (^{15}N-Leu) at position Leu8; or with both ^{15}N at Leu8 and CF_3-*L*-Bpg at either Phe4 or Ile7. The synthesized peptides are listed in Fig. 1 with sequences and the abbreviations used in this article. Standard Fmoc-solid phase synthesis protocols were used [87] on an automated Liberty 1 microwave peptide synthesizer (CEM, Kamp-Lintfort, Germany), or on an automated Syro II peptide synthesizer (MultiSynTech, Witten, Germany). Peptides were purified using C18 reverse phase HPLC columns with water/acetonitrile gradients each containing 5 mM HCl as ion pairing agent. The identity of the peptides was confirmed by an LC–MS system equipped with an 1100 Series LC-system from Agilent (Santa Clara, USA) coupled to an ESI micro-TOF mass spectrometer from Bruker Daltonics (Bremen, Germany).

2.3. Circular dichroism (CD) spectropolarimetry

The lipid powders (DMPC, DMPG) were dissolved in chloroform/methanol 50/50 (v/v) to obtain 14 mM stock solutions. Aliquots of the stock solutions were mixed in a glass vial and thoroughly vortexed to obtain the DMPC/DMPG 3:1 mixture (molar ratio). Subsequently, the organic solvents were removed under a gentle stream of nitrogen, followed by overnight vacuum. The lipid film that had formed at the

bottom of the vial was dispersed by addition of 10 mM phosphate buffer (PB, pH 7.0) and homogenized by 10 freeze–thaw cycles followed by vigorously vortexing for 1 min after each cycle. Afterward, small unilamellar vesicles (SUVs) were formed by sonication of the MLVs for 4 min in a strong ultrasonic bath (UTR 200, Hielscher, Germany). The sonication procedure was repeated 3 times, after cooling the water of the ultrasonic bath down to room temperature with ice, to avoid overheating of the samples.

To prepare the final CD samples, an aliquot of the respective 350 μM peptide stock solution in water was added to either pure 10 mM PB or to a 50/50 (v/v) mixture of TFE (2,2,2-trifluoroethanol) and 10 mM PB or to the DMPC/DMPG (3:1) liposome dispersion in 10 mM PB. The final peptide concentration was in the range 40–150 μM for the 10 mM PB solutions, 20–75 μM for the TFE/10 mM PB mixtures and in the liposome samples it was adjusted to ~20 μM, which resulted in a peptide-to-lipid molar ratio (P/L) of 1:100, given the lipid concentration of 2 mM.

CD spectra of these samples were recorded on a J-815 spectropolarimeter (JASCO, Groß-Umstadt, Germany). Measurements were performed in quartz glass cells (Suprasil, Hellma, Müllheim, Germany) of 1 mm path length between 260 and 185 nm at 0.1 nm intervals. Spectra were recorded at 20 °C for the pure PB buffer and PB/TFE mixtures, and at 30 °C for the vesicle suspensions (i.e. above the phase transition temperature of the lipids), using a water-thermostated rectangular cell holder. Three repeat scans at a scan-rate of 10 nm min^{-1}, 8 s response time and 1 nm bandwidth were averaged for each sample and for the baseline of the corresponding peptide-free sample. After subtracting the baseline spectra from the sample spectra, CD data were processed with the adaptive smoothing method, which is part of the Jasco Spectra Analysis software. Finally, the spectral data were converted to mean residue ellipticities by measuring the concentration of each peptide stock solution based on the 280 nm UV absorbance of the Tyr residue contained in the sequence [88]. The absorption spectrum in the range of the Tyr aromatic bands was recorded from 340 to 240 nm in a quartz glass half-micro-cuvette with 1 cm optical path length (Hellma, Müllheim), using 10 mM phosphate buffer as a blank. The peptide concentration was calculated from the baseline-corrected absorbance using a molar extinction coefficient of 1490 l mol^{-1} cm^{-1} for the Tyr absorption at 280 nm [88]. The concentration of the final CD samples was calculated from the respective dilution factors.

Secondary structure estimation from CD spectra was performed using the CDSSTR program with the implemented singular value decomposition (SVD) algorithm [89,90], by the CONTIN-LL program, which is based on the ridge regression algorithm [91,92], and by the SELCON-3 program, which incorporates the self-consistent method together with the SVD algorithm to assign protein secondary structure [93,94]. The three algorithms are provided by the DICHROWEB on-line server [95,96]. The quality of the fit between experimental and back-calculated spectrum corresponding to the estimated secondary structure fractions was assessed from the normalized root mean square deviation (NRMSD), with a value <0.1 (for CONTIN-LL and CDSSTR) and <0.25 (for SELOCN-3) considered as a good fit [95]. Finally, the secondary structure element fractions of each sample were calculated as the mean value of the individual data obtained with the three algorithms.

2.4. Oriented circular dichroism spectroscopy (OCD)

OCD experiments on macroscopically oriented samples were performed with a designated OCD-cell built in-house, which is computer controlled and can be integrated in our J-810 spectropolarimeter as an accessory [79]. Oriented samples of BP100-wt in DMPC/DMPG (3:1) bilayers with P/L ratios of 1:100, 1:25, and 1:12.5 were prepared from corresponding BP100-wt vesicle suspensions (for preparations of vesicles see section on CD above). For this, a 50- to 100-μl aliquot of the sample containing a maximum of 0.2 mg lipid was deposited on a quartz glass plate with a 20-mm diameter. The water of the vesicle suspension was allowed to evaporate in a gentle stream of air until the sample appeared dry (resulting in a circular spot of ~12-mm diameter). Samples were subsequently hydrated for 15 h at 30 °C in the OCD sample cell. A small volume of saturated K_2SO_4 salt solution (300–500 ml) was placed in the bottom of the cell to maintain 97% humidity. To minimize spectral artifacts (e.g. linear dichroism contributions) OCD spectra were recorded at 30 °C every 45° of rotation of the cell at eight different rotation angles [79], and referenced by subtracting the background signal that was recorded with a sample containing the same amount of lipids without peptides using the same data acquisition parameters as in the normal CD measurements.

2.5. NMR sample preparation

Oriented NMR samples were prepared by co-dissolving the lipid and peptide in suitable organic solvents, spreading the mixture on glass plates, removal of the organic solvent, and subsequent hydration. Details have been published elsewhere [50,58]. Usually 0.3 mg of ^{19}F-labeled peptide or 0.5 mg of ^{15}N-labeled peptide was used, and appropriate amounts of lipids to get the desired P/L ratio. For the 1:3000 sample 0.023 mg peptide was used.

2.6. Solid state NMR

^{31}P NMR measurements to check the sample quality and degree of lipid orientation were performed at 202.5 MHz on an Avance III Bruker NMR spectrometer (Bruker Biospin, Karlsruhe, Germany) with a wide bore 500 MHz magnet, using a Hahn echo sequence [97] with a 90° pulse of 5 μs and a 30 μs echo time, with ^{1}H SPINAL64 decoupling [98] during acquisition. Typically 256 scans were accumulated. The acquisition time was 10 ms and the recycle time 1 s.

^{19}F NMR was performed using a home-built probe head at a frequency of 470.6 MHz using an anti-ringing sequence [99] with a 90° pulse of 3.25 μs, a sweep width of 500 kHz, 4096 data points, and proton decoupling using TPPM [100]. Depending on the amount of peptide, between 10,000 and 240,000 scans were acquired. The ^{19}F chemical shift was referenced using the fluorine signal of a 100 mM solution of NaF, of which the chemical shift was set to −119.5 ppm.

^{1}H–^{15}N cross polarization experiments using a CP-MOIST pulse sequence [101] were performed at 60.8 MHz on an Avance Bruker NMR spectrometer (Bruker Biospin, Karlsruhe, Germany) with a wide bore 600 MHz magnet. The spectra were acquired using a home-built double-tuned probe with a low-E flat-coil resonator (3 mm × 9 mm cross section), employing a ^{1}H and ^{15}N radiofrequency field strength of 65 kHz during the cross polarization, and 36 kHz ^{1}H SPINAL16 decoupling during acquisition. A mixing time of 250 μs was found to be optimal, and up to 14,000 scans were accumulated. The acquisition time was 10 ms and the recycle time was 5 s. The ^{15}N chemical shift was referenced using the signal of a dry powder of ammonium sulfate, of which the chemical shift was set to 26.8 ppm. All NMR experiments were performed at 35 °C, unless otherwise stated. The temperature of the sample inside the NMR probe was calibrated using a methanol sample [102].

2.7. NMR data analysis

The orientation of a helical peptide in the membrane is defined by two angles, the tilt angle τ, defined as the angle between the long axis of the helix and the membrane normal, and the azimuthal rotation angle ρ, which defines the rotation of the peptide around its long axis. For calculating the peptide orientation and dynamics, the structure of BP100 is assumed to be an ideal α-helix, based on a poly-alanine model generated with SYBYL (Tripos, St. Louis, USA) [23]. Using ^{19}F NMR data from all six labeled positions, the helix orientation is calculated from RMSD fits and quadrupolar wave plots, as described in detail previously [40]. Previously, we have defined the ρ angle starting from

residue 12 in the sequence [23], but for BP100 we use as starting point residue 1 (This leads to a shift of ρ angles with -20°, i.e., a ρ angle here found to be 159° would with the previous definition be 179°.). Peptide dynamics were accounted for by using two different models, which have been explained in detail elsewhere [72]. Briefly, in the "implicit" dynamical model, the local and global mobility of the peptide helix is described by an order parameter S_{mol}. This term reduces all ^{19}F–^{19}F dipolar coupling by a factor between 0 and 1, where 0 means complete isotropic averaging and 1 corresponds to an immobile situation without any dynamics, except possible diffusional translation and rotation around the bilayer normal, which do not influence the splittings for peptides in membranes oriented with the bilayer normal parallel to the magnetic field. In the "explicit" model, dynamics is described as Gaussian distribution of τ and ρ angles, with widths σ_τ and σ_ρ, respectively. Larger widths correspond to a more dynamic situation, in which the angles undergo fluctuations with larger amplitudes. It is assumed that the whole-body helix fluctuations are fast on the NMR time scale, so that the measured splittings represent time-averages over these distributions [72].

3. Results

Several BP100 analogs were synthesized, either with a ^{15}N label at the backbone amide of Leu8, or with a single CF_3-Bpg side chain as a conservative replacement of Leu3, Phe4, Ile7, Leu8, Tyr10, or Leu11 as shown in Fig. 1. The ^{15}N-labels do not affect the chemical properties of the molecule, but ^{19}F-labeling might influence the biological function and/or structure of the peptide. We therefore tested the antimicrobial activity against various Gram-positive and Gram-negative strains, and found no significant difference between wild type BP100 and the six ^{19}F-labeled analogs (Table A1 in Supporting Material). We also recorded circular dichroism spectra to determine the conformation of these peptides in 10 mM PB, in TFE/10 mM PB solution, and in the presence of DMPC/DMPG (3:1) vesicles at a P/L ratio of 1:100. In phosphate buffer, BP100-wt and all ^{19}F-labeled analogs are unstructured, as seen from the random coil spectral with a typical minimum around 198 nm and mostly negative ellipticities over the full spectral range from 185 to 260 nm, as seen in Fig. 2A. All of the peptides fold as α-helices in the presence of negatively charged DMPC/DMPG (3:1) vesicles, as seen from the spectral line shapes in Fig. 2B with a positive maximum around 192 nm and two negative bands at 208 nm and 223 nm. In 50% TFE (v/v), the peptides are also α-helical (see supporting Fig. A1). A secondary structure estimation was performed from the CD spectra in the presence of DMPC/DPMG (3:1), and the secondary structure elements of the different BP100 analogs are listed in Table 1. These unusually short BP100 peptides are predominantly α-helical, with the CF_3-Bpg containing analogs showing even slightly more helix content (around 75%) than the wild type peptide (61%). Thus, the CD conformational analysis together with the antimicrobial tests confirms that CF_3-Bpg labeling of BP100 does not significantly perturb neither the secondary structure nor the biological function of the peptide.

The orientation of α-helical peptides in a membrane can be roughly assessed using oriented CD (OCD) in fully hydrated, macroscopically aligned membrane samples [79,103]. OCD experiments were performed on BP100 in DMPC/DMPG (3:1) bilayers at different P/L ratios, from moderate 1:100 up to a high peptide concentration of 1:12.5. In all cases, the OCD spectra (Fig. 3) correspond to peptides with the long axis of the α-helix parallel to the plane of the membrane, i.e. in the surface-bound state or so-called "S-state". This can be seen from the pronounced negative band around 208 nm, which has stronger intensity compared to the band around 223 nm. Moreover, from the quite similar line shape of all spectra at wavelengths >200 nm it can be inferred that there is no change in the ratio of the two bands and thus no re-orientation of the peptide at higher P/L ratios. This behavior is in contrast to longer α-helical AMPs, many of which have been found to undergo a concentration-dependent re-alignment in the membrane [40,47,50,79,104,105].

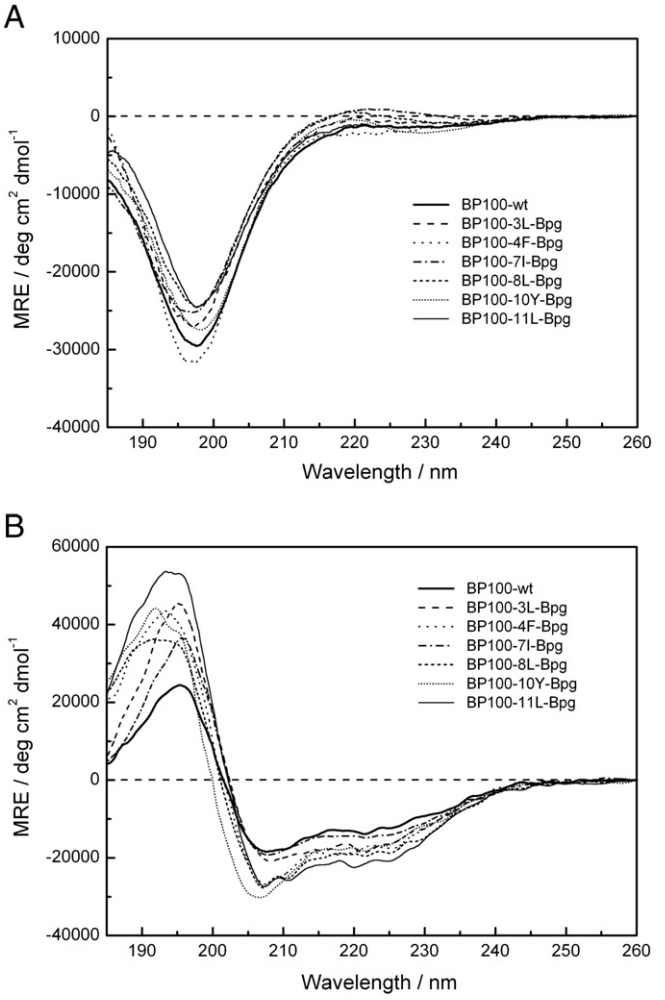

Fig. 2. CD spectra of BP100 and ^{19}F-labeled analogs in (A) 10 mM PB, and (B) in the presence of DMPC/DMPG (3:1) vesicles, P/L 1:100, 10 mM PB.

For α-helical peptides it is also possible to estimate the helix tilt angle in a membrane using ^{15}N NMR on a peptide labeled with ^{15}N in the backbone, using a macroscopically oriented sample with the bilayer normal parallel to the magnetic field. ^{15}N NMR experiments were performed on BP100 with a ^{15}N-label at Leu8 in the same kind of oriented DMPC/DMPG (3:1) bilayers as used for OCD, at P/L ratios of 1:50, 1:100 and 1:200. All three ^{15}N NMR spectra in Fig. 4 show a narrow signal at

Table 1
Secondary structure fractions of BP100-wt peptide and CF_3-Bpg-labeled analogs in DMPC/DMPG (3:1) vesicles, evaluated from the CD spectra using three different algorithms.

Sample	Fraction of secondary structure element[a]				
	α-Helix	β-Sheet	Turn	Unordered	Total
BP100-wt	0.61	0.04	0.13	0.22	1.00
BP100-3L-Bpg	0.77	0.02	0.08	0.13	1.00
BP100-4F-Bpg	0.77	0.03	0.06	0.15	1.01
BP100-7I-Bpg	0.71	0.04	0.09	0.16	1.00
BP100-8L-Bpg	0.74	0.02	0.08	0.16	1.00
BP100-10Y-Bpg	0.74	0.04	0.09	0.14	1.01
BP100-11L-Bpg	0.87	0.01	0.04	0.07	0.99

[a] Data represent mean values of the results obtained with three different secondary structure estimation algorithms. Individual results of the different analyses were not considered when the sum of all structural element fractions was <0.98 or >1.02, or when the NRMSD (normalized root mean square deviation) between the experimental and back-calculated CD spectrum was above the threshold value (0.1 for CONTIN-LL and CDSSTR, and 0.25 for SELCON-3).

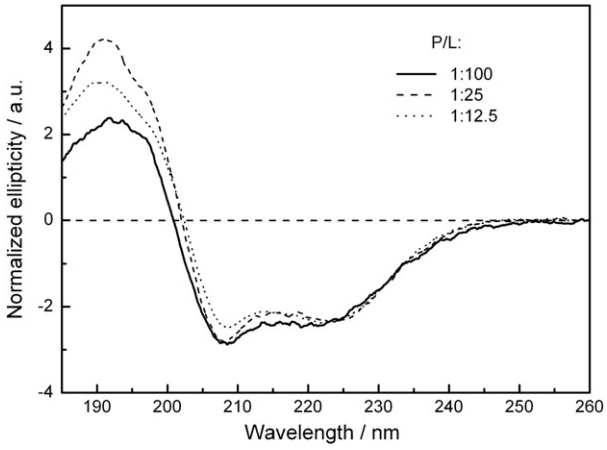

Fig. 3. Oriented CD of BP100 in DMPC/DMPG (3:1) bilayers at different peptide-to-lipid molar ratios (P/L). The spectra are normalized to the same intensity (223 nm) to illustrate the similarity in the line shapes.

92 ppm, corresponding to peptides in a surface-bound orientation (S-state) with τ close to 90° [27]. The P/L = 1:100 sample was also measured with the bilayer normal perpendicular to the magnetic field, and the signal was shifted to 135 ppm, showing that the peptide is rotating fast around the bilayer normal. This can also be seen from a hydrated multilamellar vesicle sample, where all membrane orientations are present, and which is motionally averaged compared to the dry peptide powder spectrum (see Fig. A2).

The chemical shift does not vary with the P/L ratio, indicating that the helix orientation does not change with the concentration of the peptide in the membrane, in full agreement with the OCD results. It should also be noted that to observe an NMR signal, a cross-polarization pulse sequence was used to transfer polarization from ^{1}H spins to ^{15}N spins. The best polarization transfer was found with an unusually short mixing time of 250 μs, whereas with a mixing time of 500 μs or 1000 μs no signal was observed. For longer AMPs, like the 21-mers PGLa and MSI-103, we have often used mixing times of 500–1000 μs, with longer mixing times being more suitable for the least mobile peptides (as determined from ^{2}H or ^{19}F NMR) [39,40]. On the other hand, for the small cyclic decapeptide gramicidin S, we also found that short mixing times (100–200 μs) gave the best ^{15}N NMR signal [45]. From our experience, the short mixing time of 250 μs is therefore indicative of a highly dynamical system, which implies that BP100 is very likely monomeric and rather mobile per se.

OCD and ^{15}N NMR using a single ^{15}N-label can only give an approximate tilt angle of the peptide, and the azimuthal rotation angle ρ is not available from these experiments. They do not provide much detailed information on whole-body fluctuations either, nor on a potential unraveling of the helix termini. Furthermore, neither OCD nor ^{15}N NMR is sensitive enough to address low peptide-to-lipid ratios under usual experimental conditions, as the concentration range of both methods is limited to about P/L ≥ 1:300. To obtain a more comprehensive and detailed description of the peptide structural and dynamical behavior, ^{19}F NMR is thus considered to be the method of choice [22–26,36,40–70]. To this aim, six individually ^{19}F-labeled BP100 analogs were synthesized and reconstituted in oriented bilayers of DMPC/DMPG (3:1), just as for OCD and ^{15}N NMR, but covering now a much wider range of P/L ratios from 1:3000 up to 1:10, which is accessible only by ^{19}F NMR.

The lipid orientation of samples on glass plates was checked with ^{31}P NMR, showing that lipid bilayers were well oriented, except at very high peptide concentrations above P/L ≥ 1:20 where the lipid order gets perturbed (see Fig. A3). From the ^{19}F NMR spectra shown in Fig. 5, the homonuclear ^{19}F–^{19}F dipolar coupling for each specific labeled position is obtained from the splitting of the triplet [23]. The spectra in Fig. 5A of the different Bpg-labeled peptides in lipid bilayers at P/L = 1:100 all exhibit well resolved dipolar splittings, which differ for the different positions (values are given in Table 2). The ^{19}F dipolar splittings remain almost unchanged even at high concentration (Fig. 5B), indicating that the peptide does not aggregate, in full agreement with the CD analysis. From Fig. 5B and Table 2, it is thus clear that the orientation of BP100 in the membrane does not change over the entire concentration range from a P/L of 1:3000 to 1:10. These data also confirm that the helical structure of BP100 remains unchanged (including the peptide termini) even at low concentration.

To determine whether the BP100 molecules are free to diffuse rotationally within the plane of the membrane (on the millisecond

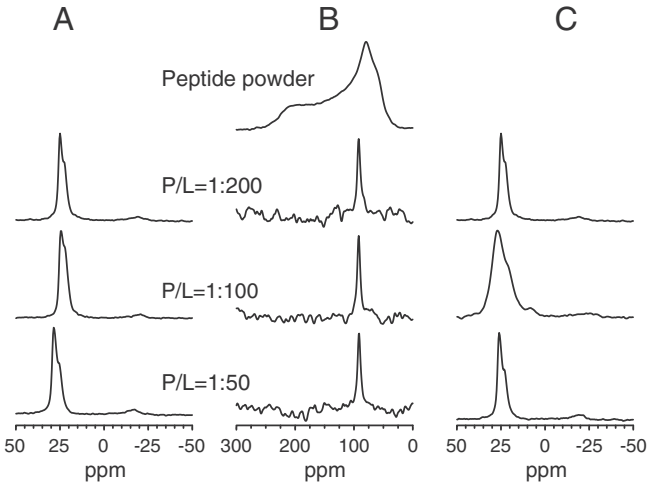

Fig. 4. Solid-state NMR spectra of BP100-8L-^{15}N in oriented bilayers of DMPC/DMPG (3:1), at three different P/L values. (A) ^{31}P NMR spectra before the ^{15}N NMR experiment. (B) ^{15}N NMR spectra. The top spectrum is from a dry peptide powder sample without lipid to illustrate the underlying chemical shift anisotropy. The chemical shift of the sharp peak in the membrane sample is in all three cases 92 ppm, indicating a surface-bound orientation of the helix. (C) ^{31}P NMR spectra after the ^{15}N NMR experiment, acquired to confirm that the sample has not dried out or deteriorated otherwise.

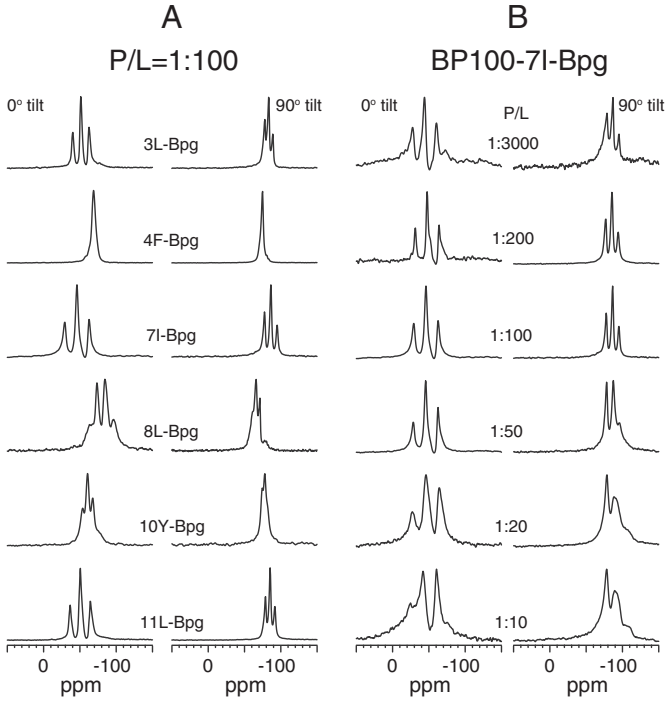

Fig. 5. (A) ^{19}F NMR spectra of oriented samples of BP100, labeled with CF_3-Bpg at different positions, in DMPC/DMPG (3:1) bilayers at P/L = 1:100. (B) ^{19}F NMR spectra of oriented samples of BP100-7I-Bpg, in DMPC/DMPG (3:1) bilayers at different P/L ratios.

Table 2
^{19}F–^{19}F dipolar couplings (in kHz) of CF_3-Bpg labeled BP100 analogs in DMPC/DMPG (3:1) bilayers.

Different peptides at P/L = 1:100			BP100-7l-Bpg at different P/L		
Peptide	0°	90°	P/L ratio	0°	90°
BP100-3L-Bpg	+5.1	−2.4	1:3000	+7.7	−3.8
BP100-4F-Bpg	+1.0	−0.5	1:200	+7.7	−4.0
BP100-7l-Bpg	+8.2	−4.1	1:100	+8.2	−4.1
BP100-8L-Bpg	−5.2	+2.5	1:50	+8.0	−4.3
BP100-10Y-Bpg	+3.2	−1.4	1:25	+8.6	−4.6
BP100-11L-Bpg	+6.5	−3.2	1:10	+8.7	−5.3

NMR time scale), two ^{19}F NMR experiments were performed for each oriented sample, by placing it with the membrane normal parallel (0°) as well as perpendicular (90°) to the external magnetic field. The spectra for both orientations are shown in Fig. 5, and the corresponding dipolar couplings are given in Table 2. The splittings measured at 90° are found to be scaled by a factor of approximately −1/2 compared to the splittings measured at 0°. This indicates a fast rotational diffusion of peptides around the bilayer normal [23], which again suggests that BP100 is highly mobile in the membrane-bound state, and monomeric like many other membrane-active peptides [23,44,47,48,50,74].

From the ^{19}F-^{19}F dipolar couplings of the different labeled positions, the conformation and orientation of a peptide can be determined as described in the Materials and methods section. For any specific values of τ and ρ angles, the couplings are calculated for a given peptide conformation. Since we know from CD and OCD that BP100 and its analogs form an α-helix in lipid bilayers, an ideal α-helical geometry was used in the ^{19}F NMR data analysis. One point of interest, especially in view of the very short BP100 sequence, is whether this structural assumption is valid all the way up to the peptide termini. Fig. 6A shows the helical wave plot of the dipolar couplings as a function of residue number. The quality of the fit is high, in the sense that the best-fit curve fits well to all experimental data points. Since none of the data points deviate from the fitted curve, we may conclude that BP100 forms a continuous and compact α-helix all the way from Leu3 to Leu11.

To obtain reliable structural results, it is usually important to take dynamics into account in the NMR data analysis of membrane-bound peptides [71–73,75,76]. We may expect that this aspect is particularly relevant for the short and compact BP100 helix, for which the ^{15}N NMR mixing time had already suggested an unusually high mobility. The ^{19}F NMR data were thus analyzed using an "explicit" dynamical model, where the dynamics are described explicitly by whole-body fluctuations of the τ and ρ angles. It is assumed that these angles fluctuate on a timescale which is fast compared to the NMR experiment, so that the ^{19}F dipolar splittings reflect averages over these fluctuations. Furthermore, this model implies that fluctuations can be described with Gaussian probability distributions of angles, i.e. by an average value τ_0 (or ρ_0) plus a width of the distribution σ_τ (or σ_ρ) [72]. The result of this advanced analysis is shown in Fig. 6 for BP100 in DMPC/DMPG (3:1) at P/L = 1:100. There is a best fit orientation corresponding to $\tau = 156°$, $\rho = 159°$, $\sigma_\tau = 3°$ and $\sigma_\rho = 3°$. In Fig. 6A and B the helical curves corresponding to these parameter values are plotted together with the experimental data points. The fit is reasonably good with a best fit RMSD = 0.83 kHz. Fig. 6C shows the RMSD as a function of τ and ρ, using a color coding. To project the four-dimensional data down to two dimensions, for each (τ,ρ) pair the lowest RMSD for any particular combination of σ_τ and σ_ρ is plotted, meaning that for each orientation (τ,ρ) the respective local (σ_τ,σ_ρ) optimum is used. These considerations now give rise to an additional plot of the RMSD as a function of σ_τ and σ_ρ, shown in Fig. 6D. Here, analogously, for each (σ_τ,σ_ρ) pair the values of τ and ρ giving the best fit in each case are used.

The global best fit gives small values of Gaussian widths σ_τ and σ_ρ, indicating at first sight that the peptide should be almost immobile.

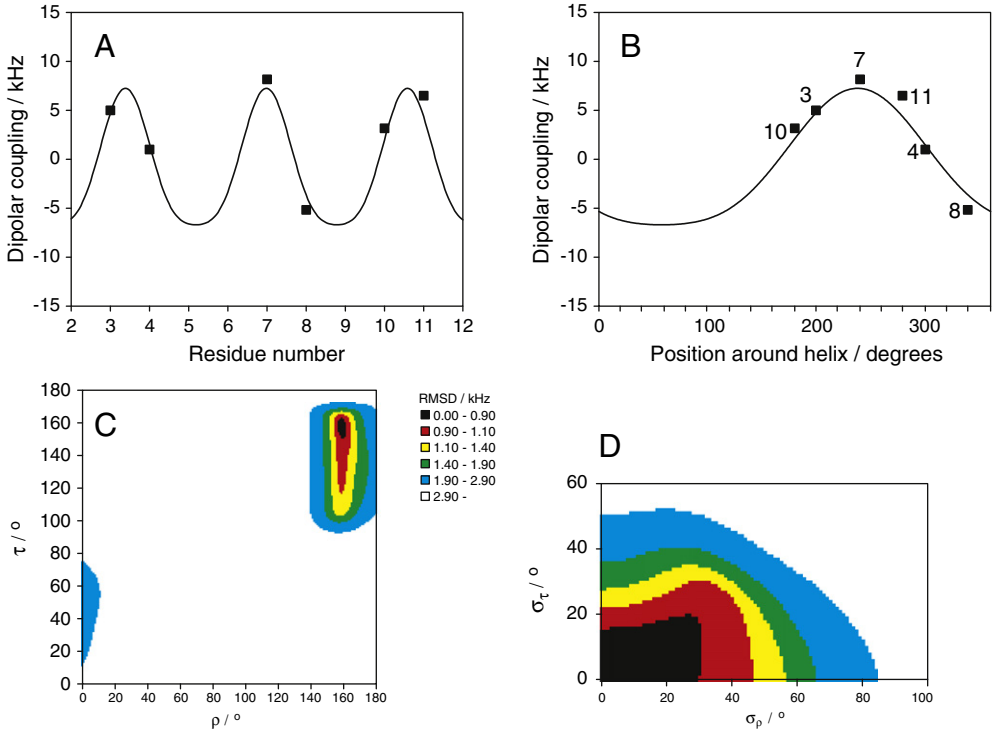

Fig. 6. Analysis of ^{19}F NMR data of BP100 in DMPC/DMPG (3:1) bilayers at P/L = 1:100 using the explicit dynamical model. (A) Best-fit helical wave plotted against dipolar couplings measured at different labeled positions in the helix. (B) The same helical wave plotted around one turn of the helix, with labeled positions marked at the angle corresponding to the position around the helix axis, according to a helical wheel view (see Fig. 1). Since all labels are on the same face of the helix, they cluster in one stretch of the helical wave. (C) RMSD between experimental and calculated splittings, for all τ and ρ values used in the calculation. For each τ-ρ pair, the best-fit values of σ_τ and σ_ρ are used, which can be different for different pairs of angles. The RMSD is color-coded, and the lowest RMSD is marked in black. The red area has an RMSD <0.3 kHz larger than the best-fit value. (D) RMSD between experimental and calculated splittings, for all σ_τ and σ_ρ values used in the calculation. For each σ_τ-σ_ρ pair, the best-fit values of τ and ρ are used, which can thus be different for different pairs of angles. The RMSD is color-coded, using the same scale as in (C), so that for example the black parts of both figures correspond to the same parameter values.

However, this solution is by no means unique or sharply defined, as a large range of τ values (from 110° to 160°) give almost the same RMSD, as seen in Fig. 6C. The global best fit has RMSD = 0.83 kHz, while the entire region in red corresponds to orientations where RMSD is still less than 1.1 kHz. All these helix tilt angles are therefore compatible with the experimental ^{19}F NMR data. Similarly, a wide range of σ_τ, and σ_ρ values are also compatible with the RMSD, as seen in Fig. 6D. We thus face an ambiguous situation in this ^{19}F NMR analysis of BP100, where the helix tilt angle has a very broad range of possible tilt angles. For the azimuthal rotation angle ρ, the best fit value is much better defined, as only the region from 155° to 165° gives an acceptable RMSD.

To narrow down the ambiguity in the tilt angle, we refer back to the ^{15}N NMR and OCD data above (Figs. 3 and 4), which had shown that BP100 is aligned essentially parallel to the membrane surface in an S-state. To be sure that the CF_3-Bpg-substitution had not affected the orientation of the ^{19}F-labeled analogs compared to BP100-wt, OCD was also performed on BP100-7I-Bpg, but there was no difference in the spectral lineshape (see Fig. A4A). As extra further control, we also prepared doubly-labeled peptides, containing both ^{15}N at Leu8 as well as CF_3-Bpg at position Leu3 or Ile7. However, no significant difference was seen between the singly-labeled and doubly-labeled peptides in either the ^{31}P, ^{15}N or ^{19}F NMR spectra, again confirming that the orientation of the peptide was not affected due to ^{19}F-labeling (see Fig. A4B and A4C), in line with the biological activity tests above (see Table A1).

If we critically reconsider the ^{19}F NMR data and accept an RMSD value of 0.3 kHz above the best-fit value of 0.8 kHz, then a tilt angle of $\tau \approx 110°$ is compatible with all the different experimental methods used. This means that the amidated, uncharged C-terminus of BP100 would point slightly deeper into the membrane than the charged N-terminus (i.e. $\tau \approx 110°$ between the membrane normal and the helix axis running from N- to C-terminus). For this very plausible solution (also in the light of the ^{15}N NMR and OCD results), we obtain corresponding values of $\rho \approx 160°$, $\sigma_\tau \approx 5°$, and $\sigma_\rho \approx 40°$ from the dynamical ^{19}F NMR analysis. We can thus reconcile all our orientational data into one comprehensive picture of BP100: The helical peptide lies almost flat on the membrane surface, with only a slightly deeper immersion of the amidated C-terminus. The azimuthal rotation angle is close to 160°, meaning that the charged Lys side chains point out of the membrane into the aqueous layer, as expected. Furthermore, the peptide is rather dynamic with a fluctuating tilt of $\sigma_\tau \geq 5°$ and a pronounced variation in $\sigma_\rho \geq 40°$.

4. Discussion

Solid-state NMR is a powerful method to determine the conformation, alignment and dynamics of peptides in oriented membrane samples. Many important insights have been obtained this way on phenomena like hydrophobic mismatch [19,20,75,106], on the role of anchoring residues in hydrophobic peptides [37,106–108], and on the mode of action of antimicrobial peptides, which have in some cases been found to be inserted in the membrane in accordance with the formation of transmembrane pores [46,109]. The general NMR approach, based on the use of selective ^{2}H- ^{15}N- or ^{19}F-labels, is routinely established for longer α-helical peptides. However, the study of short peptides, such as BP100 with only 11 amino acids, is still an unmet challenge for several reasons that will be discussed below. These include (i) the necessity of the peptide to assume a regular fold, (ii) the risk of unraveling at the termini, (iii) the limited number of positions that are suitable for selective labeling, (iv) the uneven distribution of labels over the helical wheel, and (v) the possibility that a compact molecular shape undergoes vigorous dynamics in fluid membranes.

The traditional way to analyze helical peptides with selective ^{2}H- or ^{19}F-labels in the side chains is based on the GALA approach (geometric analysis of labeled alanines) [19,20,38,47,50,58,74–76,105,106,108,109]. In previous studies, peptides had a typical length of around 20 amino acids, and the labels could be placed along the central stretch of the peptide, far from the termini where unfolding or non-ideal helix geometries may occur. Notably, it was shown for the transmembrane peptide GWALP23 that the data from labels in positions 3 and 21 does not fit to a helical wave determined from the central positions 7–17 [37], indicating a partial unfolding of the helix beyond the flanking Trp residues at either end. Also in the case of the amphiphilic surface-bound peptide PGLa, the label at position 20 (out of 21 amino acids) did not fit well to the helical wave based on the central stretch at P/L = 1:200 in DMPC, while at P/L = 1:50 there was a good match [104]. These observations raise the question whether and to what extent membrane-bound peptides may have a tendency to unravel at their termini.

Our CD analysis of BP100 showed that this membrane-bound peptide is highly α-helical, hence it fulfills the first of the above criteria (i) to allow a more detailed solid-state NMR structure analysis. Deconvolution of the CD data gave up to 87% helix content (Table 1), suggesting that only 1–2 amino acids at the termini may not be folded properly. It was indeed possible to fit a helical wave to all of the data points measured from six ^{19}F-labels between positions 3 and 11 (Fig. 6A), which alleviates the second challenge (ii). OCD showed that BP100 is oriented approximately flat on the membrane surface (Fig. 3), and the same helix alignment was estimated from the NMR signal of a single ^{15}N-label in the middle of the sequence (Fig. 4). To obtain further details on the azimuthal rotation and the dynamical behavior of BP100, a comprehensive ^{19}F-NMR analysis was performed using six CF_3-Bpg labels. In previous studies with a similar number of data points, this approach had yielded highly accurate values for both τ and ρ. However, in the case of BP100, an additional problem was encountered due to the fact that there are only very limited possibilities available for ^{19}F-labeling, as in challenge (iii). Out of the 11 amino acids in BP100, there are only six hydrophobic positions that can be labeled with CF_3-Bpg (Leu3, Phe4, Ile7, Leu8, Tyr10, Leu11). The remaining five residues are all charged, hence they are no good candidates for labeling with CF_3-Bpg because a reduction in the net charge of a peptide can reduce its antimicrobial activity and increase hemolytic side-effects [11,110].

All ^{19}F-labels are located on the same face of the amphiphilic BP100 helix (Fig. 1), which turns out to be a major challenge (iv). A lack of labels on one face of the helix may under some circumstances dramatically reduce the informative value that can be extracted from the helical wheel analysis, as is found to be the case here with BP100. The general effect of having only half the sector labeled is analyzed in more detail in the Supporting Information (Appendix B). As illustrated in Fig. 7, some

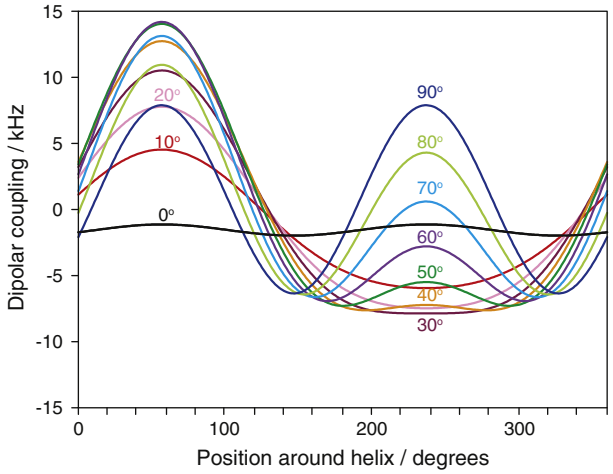

Fig. 7. Helical waves for different tilt angles, generated for a hypothetical BP100-like peptide with $\rho = 160°$, $\sigma_\tau = 10°$, and $\sigma_\rho = 20°$; the tilt angle is given in the figure next to the corresponding curve. For small tilt angles (10–30°), the region around 50° is most sensitive to changes in τ, while for large tilt angles (40–80°), the region around 240° is most sensitive.

regions of the helical wave are more characteristic and contain more critical information about the helix tilt angle than other regions. If a sector of only 180° is labeled, this may in some cases be sufficient to get a reliable fit, but not in others, so we cannot state a priori that the labeling of an amphiphilic helix will not give an accurate orientation. The degree of uncertainty in determining the helix tilt angle depends on which part of the helical wave is accessible for labeling, and on the actual alignment of the helix in the membrane. In the case of surface-bound BP100, all ^{19}F-labels happen to be located in the less informative region of the helical wave, so the analysis suffers from considerable uncertainty in the value of τ. It is obvious that for optimal results, the NMR labels should be distributed as evenly as possible around the helix axis, which will result in a unique solution with minimal uncertainty. This is easily achieved in uniformly hydrophobic transmembrane sequences, but more difficult for amphiphilic peptides, especially when they are as short as BP100. As demonstrated in Appendix B, it would be enough to have just one additional data point from the polar face of this helix to get a reliable tilt angle for BP100. So far, there are no ^{19}F NMR reporter groups available with charged side chains, but several new hydrophobic and polar ^{19}F-labels have been recently custom-designed for ^{19}F NMR structure analysis based on a cyclobutane geometry [55,56]. There is hope that the same framework may be suitable to generate charged side chains carrying a CF_3-reporter group, which would resolve challenges (iii) and (iv) by providing further data on the polar face of the helix.

We conclude that in the present case of BP100 the ^{19}F NMR analysis must be accompanied by additional experiments such as ^{15}N NMR and OCD, to narrow down the ambiguity in the helix tilt angle. Nevertheless, ^{19}F NMR has provided valuable information on the azimuthal angle, $\rho = 160°$, indicating that the charged lysine side chains of BP100 point out of the membrane. Also, the range of compatible τ-values suggests that the amidated C-terminus is slightly more inserted into the membrane than the charged N-terminus. Furthermore, we find that the peptide is very mobile, with pronounced fluctuations in the azimuthal angle ($\sigma_\rho \geq 40°$). This value is considerably higher than $\sigma_\rho \approx 20°$ found for the longer amphiphilic peptides PGLa and MSI-103 which were studied previously [72,74]. This finding indicates that BP100 does not form oligomers in the membrane, but remains monomeric up to high peptide-to-lipid ratios. Such dynamical information is not conclusively available from ^{15}N NMR or OCD. In Table 3 we give an overview of the different methods used here for BP100, and on the information that can be gained from each method.

To address challenge (v), i.e. the short peptide may be vigorously dynamic in the membrane, we used an advanced dynamical model in the data analysis. In our previous, in-depth analyses of the amphipathic α-helical peptides PGLa and MSI-103 there were no discrepancies between the ^{19}F NMR and OCD results, nor with ^{2}H NMR and ^{15}N NMR [40,47,50,79,105]. It was even possible to largely ignore the dynamics of these long amphiphilic peptides, by using a simple S_{mol} model to analyze the NMR data [72,74]. This "implicit" model gave essentially the same τ and ρ values as the more advanced dynamical model that had to be applied here to the highly mobile BP100. In the implicit model, a uniform averaging of the dipolar couplings is applied to all labeled positions, using the same scaling factor S_{mol} (which can take a value between 0 and 1). Interestingly, it was shown that this method grossly underestimated the tilt angle of the highly mobile transmembrane peptides of the WALP family [72,75,111], while it worked well for longer and less mobile amphipathic helices like PGLa [72]. We also tried to analyze the BP100 data using the implicit dynamic model (Fig. A5), which showed a well-defined RMSD minimum that describes a steeply tilted and completely immobile peptide ($\tau = 154°$, $\rho = 159°$, $S_{mol} = 1.00$). This picture is clearly incompatible with the OCD and ^{15}N NMR results and with all the information about peptide dynamics that we obtained here from ^{19}F NMR and from the mixing times used in ^{15}N NMR. The simplified analysis did not give any indication that there is a problem due to the distribution of the labels on the helical wheel, so is clearly not advisable to rely on the implicit dynamical analysis without complementary data from other methods, when the peptide is short and/or highly mobile.

Short membrane-active peptides have been in the focus of research not only in view of their cost-efficient production, but also because they pose intriguing questions concerning their mechanism of action. The short multifunctional peptide BP100 is known to have a high antimicrobial and cell penetrating activity, but is not long enough to span the lipid bilayer to form transmembrane pores. Our solid-state NMR and OCD data showed that the surface-bound amphiphilic helix does not undergo a concentration-dependent re-alignment in the membrane over a wide range of peptide-lipid ratios from 1:3000 up to 1:10. This makes an interesting contrast to the behavior of many other, longer membrane-active peptides, which have been found to bind flat to the membrane surface only at low concentration. With increasing concentration they tend to get flipped into a tilted T-state, and they can even assume a membrane-inserted I-state with an upright alignment that implicates the formation of transmembrane pores. Our results on BP100 are instead compatible with the view that these compact and highly charged surface-bound helices can damage bacterial membranes via the so-called "carpet" mechanism, whereby membranes are permeabilized by peptides without the need for pore formation. A good indication for this mechanism is seen from the ^{31}P NMR data (see Fig. A3), which shows a considerable disturbance of the lipid bilayer at high peptide concentration. However, further studies are needed to understand how the very same peptide can act on the one hand as an antimicrobial membrane-permeabilizing agent, and on the other hand as an efficient cell penetrating carrier without causing leakage in eukaryotic cells or causing significant toxic or hemolytic side effects.

Table 3
Overview of methods used to study membrane-bound BP 100 and information obtained.

Method	Helicity	Helix tilt angle	Azimuthal angle	Mobility	P/L range	Price
Solution CD[a]	✓	–	–	–	1:10–1:300	$
Oriented CD[a]	✓	✓	–	–	1:10–1:300	$
^{15}N NMR (1 label)	–	✓	–	–	1:10–1:300	$$
^{19}F NMR (6 labels)	✓	(✓)[b]	✓	✓	1:10–1:3000	$$$

[a] Circular dichroism is highly valuable to reveal β-sheet formation, which is often associated with peptide aggregation, but which was not observed for BP100.
[b] Tilt angles can be determined with high accuracy provided the labels are favorably distributed around the helix (see Appendix B).

Acknowledgments

We acknowledge the DFG-Center for Functional Nanostructures for financially supporting the NMR infrastructure (TP E1.2). We thank Andrea Eisele and Kerstin Scheubeck for the technical support with peptide synthesis, and Dr. Pavel Mykhailiuk and Prof. Igor Komarov from the National Taras Shevchenko University of Kyiv, Ukraine, for custom-synthesis of the amino acid CF_3-Bpg. We thank Prof. Jakob Ulmschneider at Shanghai Jiao Tong University and Prof. Miguel A. R. B. Castanho and his coworkers at the University of Lisbon for the fruitful discussions.

Appendices A and B. Supplementary data

Supplementary data to this article can be found online at http://dx.doi.org/10.1016/j.bbamem.2013.11.001.

References

[1] K.A. Brogden, Antimicrobial peptides: pore formers or metabolic inhibitors in bacteria? Nat. Rev. Microbiol. 3 (2005) 238–250.
[2] H.G. Boman, Antibacterial peptides: key components needed in immunity, Cell 65 (1991) 205–207.

[3] A. Peschel, H.G. Sahl, The co-evolution of host cationic antimicrobial peptides and microbial resistance, Nat. Rev. Microbiol. 4 (2006) 529–536.
[4] N. Papo, Y. Shai, Can we predict biological activity of antimicrobial peptides from their interactions with model phospholipid membranes? Peptides 24 (2003) 1693–1703.
[5] H.G. Boman, Antibacterial peptides: basic facts and emerging concepts, J. Int. Med. 254 (2003) 197–215.
[6] D.I. Fernandez, J.D. Gehman, F. Separovic, Membrane interactions of antimicrobial peptides from Australian frogs, Biochim. Biophys. Acta 1788 (2009) 1630–1638.
[7] F. Pinheiro da Silva, M.C. Machado, Antimicrobial peptides: clinical relevance and therapeutic implications, Peptides 36 (2012) 308–314.
[8] E. Badosa, R. Ferre, M. Planas, L. Feliu, E. Besalu, J. Cabrefiga, E. Bardaji, E. Montesinos, A library of linear undecapeptides with bactericidal activity against phytopathogenic bacteria, Peptides 28 (2007) 2276–2285.
[9] D. Andreu, J. Ubach, A. Boman, B. Wahlin, D. Wade, R.B. Merrifield, H.G. Boman, Shortened cecropin A-melittin hybrids. Significant size reduction retains potent antibiotic activity, FEBS Lett. 296 (1992) 190–194.
[10] L. Cavallarin, D. Andreu, B. San Segundo, Cecropin A-derived peptides are potent inhibitors of fungal plant pathogens, Mol. Plant Microbe Interact. 11 (1998) 218–227.
[11] R. Ferre, E. Badosa, L. Feliu, M. Planas, E. Montesinos, E. Bardaji, Inhibition of plant-pathogenic bacteria by short synthetic cecropin A-melittin hybrid peptides, Appl. Environ. Microbiol. 72 (2006) 3302–3308.
[12] C.S. Alves, M.N. Melo, H.G. Franquelim, R. Ferre, M. Planas, L. Feliu, E. Bardaji, W. Kowalczyk, D. Andreu, N.C. Santos, M.X. Fernandes, M.A. Castanho, *Escherichia coli* cell surface perturbation and disruption induced by antimicrobial peptides BP100 and pepR, J. Biol. Chem. 285 (2010) 27536–27544.
[13] K. Eggenberger, C. Mink, P. Wadhwani, A.S. Ulrich, P. Nick, Using the peptide BP100 as a cell-penetrating tool for the chemical engineering of actin filaments within living plant cells, ChemBioChem 12 (2011) 132–137.
[14] M. Zasloff, Magainins, a class of antimicrobial peptides from *Xenopus* skin: isolation, characterization of two active forms, and partial cDNA sequence of a precursor, Proc. Natl. Acad. Sci. U. S. A. 84 (1987) 5449–5453.
[15] K. Richter, H. Aschauer, G. Kreil, Biosynthesis of peptides in the skin of *Xenopus laevis*: isolation of novel peptides predicted from the sequence of cloned cDNAs, Peptides 6 (Suppl. 3) (1985) 17–21.
[16] J. Blazyk, R. Wiegand, J. Klein, J. Hammer, R.M. Epand, R.F. Epand, W.L. Maloy, U.P. Kari, A novel linear amphipathic β-sheet cationic antimicrobial peptide with enhanced selectivity for bacterial lipids, J. Biol. Chem. 276 (2001) 27899–27906.
[17] P. Yang, A. Ramamoorthy, Z. Chen, Membrane orientation of MSI-78 measured by sum frequency generation vibrational spectroscopy, Langmuir 27 (2011) 7760–7767.
[18] D.I. Fernandez, A.P. Le Brun, T.H. Lee, P. Bansal, M.I. Aguilar, M. James, F. Separovic, Structural effects of the antimicrobial peptide maculatin 1.1 on supported lipid bilayers, Eur. Biophys. J. 42 (2013) 47–59.
[19] E. Strandberg, S. Özdirekcan, D.T.S. Rijkers, P.C.A. Van der Wel, R.E. Koeppe II, R.M.J. Liskamp, J.A. Killian, Tilt angles of transmembrane model peptides in oriented and non-oriented lipid bilayers as determined by ^{2}H solid state NMR, Biophys. J. 86 (2004) 3709–3721.
[20] P.C.A. Van der Wel, E. Strandberg, J.A. Killian, R.E. Koeppe II, Geometry and intrinsic tilt of a tryptophan-anchored transmembrane α-helix determined by ^{2}H NMR, Biophys. J. 83 (2002) 1479–1488.
[21] R.W. Glaser, M. Grüne, C. Wandelt, A.S. Ulrich, Structure analysis of a fusogenic peptide sequence from the sea urchin fertilization protein bindin, Biochemistry 38 (1999) 2560–2569.
[22] S. Afonin, R.W. Glaser, M. Berditchevskaia, P. Wadhwani, K.H. Guhrs, U. Mollmann, A. Perner, A.S. Ulrich, 4-Fluorophenylglycine as a label for ^{19}F-NMR structure analysis of membrane-associated peptides, ChemBioChem 4 (2003) 1151–1163.
[23] R.W. Glaser, C. Sachse, U.H.N. Dürr, P. Wadhwani, A.S. Ulrich, Orientation of the antimicrobial peptide PGLa in lipid membranes determined from ^{19}F-NMR dipolar couplings of 4-CF_3-phenylglycine labels, J. Magn. Reson. 168 (2004) 153–163.
[24] E. Strandberg, A.S. Ulrich, NMR methods for studying membrane-active antimicrobial peptides, Concepts Magn. Reson. A 23A (2004) 89–120.
[25] A.S. Ulrich, Solid state ^{19}F-NMR methods for studying biomembranes, Prog. Nucl. Magn. Reson. Spectrosc. 46 (2005) 1–21.
[26] S.L. Grage, J.B. Salgado, U.H.N. Dürr, S. Afonin, R.W. Glaser, A.S. Ulrich, Solid state ^{19}F-NMR of biomembranes, in: S.R. Kiihne, H.J.M. deGroot (Eds.), Perspectives on Solid State NMR in Biology, vol. 1, Kluwer Academic Publishers, Dordrecht/Boston/London, 2001, pp. 83–91.
[27] B. Bechinger, Y. Kim, L.E. Chirlian, J. Gesell, J.M. Neumann, M. Montal, J. Tomich, M. Zasloff, S.J. Opella, Orientations of amphipathic helical peptides in membrane bilayers determined by solid-state NMR spectroscopy, J. Biomol. NMR 1 (1991) 167–173.
[28] J. Wang, J. Denny, C. Tian, S. Kim, Y. Mo, F. Kovacs, Z. Song, K. Nishimura, Z. Gan, R. Fu, J.R. Quine, T.A. Cross, Imaging membrane protein helical wheels, J. Magn. Reson. 144 (2000) 162–167.
[29] F.M. Marassi, S.J. Opella, A solid-state NMR index of helical membrane protein structure and topology, J. Magn. Reson. 144 (2000) 150–155.
[30] M.S. Balla, J.H. Bowie, F. Separovic, Solid-state NMR study of antimicrobial peptides from Australian frogs in phospholipid membranes, Eur. Biophys. J. 33 (2004) 109–116.
[31] I. Marcotte, K.L. Wegener, Y.H. Lam, B.C. Chia, M.R. de Planque, J.H. Bowie, M. Auger, F. Separovic, Interaction of antimicrobial peptides from Australian amphibians with lipid membranes, Chem. Phys. Lipids 122 (2003) 107–120.
[32] A. Naito, Structure elucidation of membrane-associated peptides and proteins in oriented bilayers by solid-state NMR spectroscopy, Solid State Nucl. Magn. Reson. 36 (2009) 67–76.
[33] A. Ramamoorthy, D.K. Lee, T. Narasimhaswamy, R.P.R. Nanga, Cholesterol reduces pardaxin's dynamics — a barrel-stave mechanism of membrane disruption investigated by solid-state NMR, Biochim. Biophys. Acta 1798 (2010) 223–227.
[34] S. Thennarasu, A. Tan, R. Penumatchu, C.E. Shelburne, D.L. Heyl, A. Ramamoorthy, Antimicrobial and membrane disrupting activities of a peptide derived from the human cathelicidin antimicrobial peptide LL37, Biophys. J. 98 (2010) 248–257.
[35] S. Toraya, K. Nishimura, A. Naito, Dynamic structure of vesicle-bound melittin in a variety of lipid chain lengths by solid-state NMR, Biophys. J. 87 (2004) 3323–3335.
[36] O. Toke, R.D. O'Connor, T.K. Weldeghiorghis, W.L. Maloy, R.W. Glaser, A.S. Ulrich, J. Schaefer, Structure of $(KIAGKIA)_3$ aggregates in phospholipid bilayers by solid-state NMR, Biophys. J. 87 (2004) 675–687.
[37] V.V. Vostrikov, A.E. Daily, D.V. Greathouse, R.E. Koeppe II, Charged or aromatic anchor residue dependence of transmembrane peptide tilt, J. Biol. Chem. 285 (2010) 31723–31730.
[38] V.V. Vostrikov, C.V. Grant, A.E. Daily, S.J. Opella, R.E. Koeppe II, Comparison of "Polarization Inversion with Spin Exchange at Magic Angle" and "Geometric Analysis of Labeled Alanines" methods for transmembrane helix alignment, J. Am. Chem. Soc. 130 (2008) 12584–12585.
[39] E. Strandberg, J. Zerweck, P. Wadhwani, A.S. Ulrich, Synergistic insertion of antimicrobial magainin-family peptides in membranes depends on the lipid spontaneous curvature, Biophys. J. 104 (2013) L9–L11.
[40] R.W. Glaser, C. Sachse, U.H.N. Dürr, S. Afonin, P. Wadhwani, E. Strandberg, A.S. Ulrich, Concentration-dependent realignment of the antimicrobial peptide PGLa in lipid membranes observed by solid-state ^{19}F-NMR, Biophys. J. 88 (2005) 3392–3397.
[41] D. Grasnick, U. Sternberg, E. Strandberg, P. Wadhwani, A.S. Ulrich, Irregular structure of the HIV fusion peptide in membranes demonstrated by solid-state NMR and MD simulations, Eur. Biophys. J. 40 (2011) 529–543.
[42] K. Koch, S. Afonin, M. Ieronimo, M. Berditsch, A.S. Ulrich, Solid-state ^{19}F-NMR of peptides in native membranes, Top. Curr. Chem. 306 (2012) 89–118.
[43] M. Ieronimo, S. Afonin, K. Koch, M. Berditsch, P. Wadhwani, A.S. Ulrich, ^{19}F NMR analysis of the antimicrobial peptide PGLa bound to native cell membranes from bacterial protoplasts and human erythrocytes, J. Am. Chem. Soc. 132 (2010) 8822–8824.
[44] D. Maisch, P. Wadhwani, S. Afonin, C. Böttcher, B. Koksch, A.S. Ulrich, Chemical labeling strategy with (R)- and (S)-triofluoromethylalanin for solid state ^{19}F NMR analysis of peptaibols in membranes, J. Am. Chem. Soc. 131 (2009) 15596–15597.
[45] S. Afonin, U.H.N. Dürr, P. Wadhwani, J.B. Salgado, A.S. Ulrich, Solid state NMR structure analysis of the antimicrobial peptide gramicidin S in lipid membranes: concentration-dependent re-alignment and self-assembly as a β-barrel, Top. Curr. Chem. 273 (2008) 139–154.
[46] S. Afonin, S.L. Grage, M. Ieronimo, P. Wadhwani, A.S. Ulrich, Temperature-dependent transmembrane insertion of the amphiphilic peptide PGLa in lipid bilayers observed by solid state ^{19}F-NMR spectroscopy, J. Am. Chem. Soc. 130 (2008) 16512–16514.
[47] E. Strandberg, N. Kanithasen, J. Bürck, P. Wadhwani, D. Tiltak, O. Zwernemann, A.S. Ulrich, Solid state NMR analysis comparing the designer-made antibiotic MSI-103 with its parent peptide PGLa in lipid bilayers, Biochemistry 47 (2008) 2601–2616.
[48] P. Wadhwani, J. Bürck, E. Strandberg, C. Mink, S. Afonin, A.S. Ulrich, Using a sterically restrictive amino acid as a ^{19}F-NMR label to monitor and control peptide aggregation in membranes, J. Am. Chem. Soc. 130 (2008) 16515–16517.
[49] S. Afonin, P.K. Mikhailiuk, I.V. Komarov, A.S. Ulrich, Evaluating the amino acid CF_3-bicyclopentylglycine as a new label for solid-state ^{19}F-NMR structure analysis of membrane-bound peptides, J. Pept. Sci. 13 (2007) 614–623.
[50] E. Strandberg, P. Wadhwani, P. Tremouilhac, U.H.N. Dürr, A.S. Ulrich, Solid-state NMR analysis of the PGLa peptide orientation in DMPC bilayers: structural fidelity of ^{2}H-labels versus high sensitivity of ^{19}F-NMR, Biophys. J. 90 (2006) 1676–1686.
[51] A.S. Ulrich, P. Wadhwani, U.H.N. Dürr, S. Afonin, R.W. Glaser, E. Strandberg, P. Tremouilhac, C. Sachse, M. Berditchevskaia, S.L. Grage, Solid-state ^{19}F-nuclear magnetic resonance analysis of membrane-active peptides, in: A. Ramamoorthy (Ed.), NMR Spectroscopy of Biological Solids, CRC Press, Boca Raton, FL, 2006, pp. 215–236.
[52] S. Afonin, U.H.N. Dürr, R.W. Glaser, A.S. Ulrich, Boomerang'-like insertion of a fusogenic peptide in a lipid membrane revealed by solid-state ^{19}F NMR, Magn. Reson. Chem. 42 (2004) 195–203.
[53] P. Wadhwani, E. Strandberg, Structure analysis of membrane-active peptides using ^{19}F-labeled amino acids and solid-state NMR, in: I. Ojima (Ed.), Fluorine in Medicinal Chemistry and Chemical Biology, Blackwell Publishing, London, 2009, pp. 463–493.
[54] P. Wadhwani, J. Reichert, E. Strandberg, J. Burck, J. Misiewicz, S. Afonin, N. Heidenreich, S. Fanghanel, P.K. Mykhailiuk, I.V. Komarov, A.S. Ulrich, Stereochemical effects on the aggregation and biological properties of the fibril-forming peptide $[KIGAKI]_3$ in membranes, Phys. Chem. Chem. Phys. 15 (2013) 8962–8971.
[55] A.N. Tkachenko, P.K. Mykhailiuk, S. Afonin, D.S. Radchenko, V.S. Kubyshkin, A.S. Ulrich, I.V. Komarov, A ^{19}F NMR label to substitute polar amino acids in peptides: a CF_3-substituted analogue of serine and threonine, Angew. Chem. Int. Ed. 52 (2013) 1486–1489.
[56] A.N. Tkachenko, D.S. Radchenko, P.K. Mykhailiuk, S. Afonin, A.S. Ulrich, I.V. Komarov, Design, synthesis, and application of a trifluoromethylated phenylalanine analogue as a label to study peptides by solid-state ^{19}F NMR spectroscopy, Angew. Chem. Int. Ed. 52 (2013) 6504–6507.
[57] V.S. Kubyshkin, P.K. Mykhailiuk, S. Afonin, S.L. Grage, I.V. Komarov, A.S. Ulrich, Incorporation of labile trans-4,5-difluoromethanoproline into a peptide as a stable label for ^{19}F NMR structure analysis, J. Fluorine Chem. 152 (2013) 136–143.
[58] P. Wadhwani, E. Strandberg, N. Heidenreich, J. Bürck, S. Fanghänel, A.S. Ulrich, Self-assembly of flexible β-strands into immobile amyloid-like β-sheets in

membranes as revealed by solid-state ^{19}F NMR, J. Am. Chem. Soc. 134 (2012) 6512–6515.
[59] V.S. Kubyshkin, P.K. Mykhailiuk, S. Afonin, A.S. Ulrich, I.V. Komarov, Incorporation of cis- and trans-4,5-difluoromethanoprolines into polypeptides, Org. Lett. 14 (2012) 5254–5257.
[60] V.S. Kubyshkin, I.V. Komarov, S. Afonin, P.K. Mykhailiuk, S.L. Grage, A.S. Ulrich, Trifluoromethyl-substituted α-amino acids as solid state ^{19}F-NMR labels for structural studies of membrane-bound peptides, in: V. Gouverneur, K. Müller (Eds.), Fluorine in Pharmaceutical and Medicinal Chemistry: From Biophysical Aspects to Clinical Applications, Imperial College Press, 2012, pp. 91–138.
[61] M. Salwiczek, P.K. Mikhailiuk, S. Afonin, I.V. Komarov, A.S. Ulrich, B. Koksch, Compatibility of the conformationally rigid CF_3-Bpg side chain with the hydrophobic coiled-coil interface, Amino Acids 39 (2010) 1589–1593.
[62] P.K. Mykhailiuk, N.M. Voievoda, S. Afonin, A.S. Ulrich, I.V. Komarov, An optimized protocol for the multigram synthesis of 3-(trifluoromethyl)bicyclo[1.1.1]pent-1-ylglycine (CF_3-Bpg), J. Fluorine Chem. 131 (2010) 217–220.
[63] S.L. Grage, S. Afonin, A.S. Ulrich, Dynamic transitions of membrane active peptides, in: A. Giuliani, A.C. Rinaldi (Eds.), Antimicrobial Peptides. Methods and Protocols, vol. 618, Springer, Humana Press, New York, 2010, pp. 183–209.
[64] P.K. Mykhailiuk, S. Afonin, G.V. Palamarchuk, O.V. Shishkin, A.S. Ulrich, I.V. Komarov, Synthesis of trifluoromethyl-substituted proline analogues as ^{19}F NMR labels for peptides in the polyproline II conformation, Angew. Chem. Int. Ed. 47 (2008) 5765–5767.
[65] P.K. Mykhailiuk, S. Afonin, A.S. Ulrich, I.V. Komarov, Convenient route to trifluoromethyl-substituted cyclopropane derivatives, Synthesis (2008) 1757–1760.
[66] U.H.N. Dürr, S.L. Grage, R. Witter, A.S. Ulrich, Solid state ^{19}F NMR parameters of fluorine-labeled amino acids. Part I: aromatic substituents, J. Magn. Reson. 191 (2008) 7–15.
[67] S.L. Grage, U.H.N. Dürr, S. Afonin, P.K. Mikhailiuk, I.V. Komarov, A.S. Ulrich, Solid state ^{19}F NMR parameters of fluorine-labeled amino acids. Part II: aliphatic substituents, J. Magn. Reson. 191 (2008) 16–23.
[68] P.K. Mikhailiuk, S. Afonin, A.N. Chernega, E.B. Rusanov, M.O. Platonov, G.G. Dubinina, M. Berditsch, A.S. Ulrich, I.V. Komarov, Conformationally rigid trifluoromethyl-substituted α-amino acid designed for peptide structure analysis by solid-state ^{19}F NMR spectroscopy, Angew. Chem. Int. Ed. 45 (2006) 5659–5661.
[69] R. Witter, F. Nozirov, U. Sternberg, T.A. Cross, A.S. Ulrich, R. Fu, Solid-state ^{19}F NMR spectroscopy reveals that Trp41 participates in the gating mechanism of the M2 proton channel of influenza A virus, J. Am. Chem. Soc. 130 (2008) 918–924.
[70] U. Sternberg, M. Klipfel, S.L. Grage, R. Witter, A.S. Ulrich, Calculation of fluorine chemical shift tensors for the interpretation of oriented ^{19}F-NMR spectra of gramicidin A in membranes, Phys. Chem. Chem. Phys. 11 (2009) 7048–7060.
[71] S. Esteban-Martín, E. Strandberg, J. Salgado, A.S. Ulrich, Solid state NMR analysis of peptides in membranes: influence of dynamics and labeling scheme, Biochim. Biophys. Acta 1798 (2010) 252–257.
[72] E. Strandberg, S. Esteban-Martín, J. Salgado, A.S. Ulrich, Orientation and dynamics of peptides in membranes calculated from ^{2}H-NMR data, Biophys. J. 96 (2009) 3223–3232.
[73] S. Esteban-Martín, E. Strandberg, G. Fuertes, A.S. Ulrich, J. Salgado, Influence of whole-body dynamics on ^{15}N PISEMA NMR spectra of membrane peptides: a theoretical analysis, Biophys. J. 96 (2009) 3233–3241.
[74] E. Strandberg, D. Tiltak, S. Ehni, P. Wadhwani, A.S. Ulrich, Lipid shape is a key factor for membrane interactions of amphipathic helical peptides, Biochim. Biophys. Acta 1818 (2012) 1764–1776.
[75] E. Strandberg, S. Esteban-Martin, A.S. Ulrich, J. Salgado, Hydrophobic mismatch of mobile transmembrane helices: merging theory and experiments, Biochim. Biophys. Acta 1818 (2012) 1242–1249.
[76] S.L. Grage, E. Strandberg, P. Wadhwani, S. Esteban-Martin, J. Salgado, A.S. Ulrich, Comparative analysis of the orientation of transmembrane peptides using solid-state ^{2}H- and ^{15}N-NMR: mobility matters, Eur. Biophys. J. 41 (2012) 475–482.
[77] Y. Wu, H.W. Huang, G.A. Olah, Method of oriented circular dichroism, Biophys. J. 57 (1990) 797–806.
[78] R. Heinzmann, S.L. Grage, C. Schalck, J. Bürck, Z. Banoczi, O. Toke, A.S. Ulrich, A kinked antimicrobial peptide from *Bombina maxima*. II. Behavior in phospholipid bilayers, Eur. Biophys. J. 40 (2011) 463–470.
[79] J. Bürck, S. Roth, P. Wadhwani, S. Afonin, N. Kanithasen, E. Strandberg, A.S. Ulrich, Conformation and membrane orientation of amphiphilic helical peptides by oriented circular dichroism, Biophys. J. 95 (2008) 3872–3881.
[80] C. Lange, S.D. Müller, T.H. Walther, J. Bürck, A.S. Ulrich, Structure analysis of the protein translocating channel TatA in membranes using a multi-construct approach, Biochim. Biophys. Acta 1768 (2007) 2627–2634.
[81] O.V. Nolandt, T.H. Walther, S. Roth, J. Bürck, A.S. Ulrich, Structure analysis of the membrane protein $TatC_d$ from the Tat system of *B. subtilis* by circular dichroism, Biochim. Biophys. Acta 1788 (2009) 2238–2244.
[82] C. Muhle-Goll, S. Hoffmann, S. Afonin, S.L. Grage, A.A. Polyansky, D. Windisch, M. Zeitler, J. Bürck, A.S. Ulrich, Hydrophobic matching controls the tilt and stability of the dimeric platelet-derived growth factor receptor (PDGFR) β transmembrane segment, J. Biol. Chem. 287 (2012) 26178–26186.
[83] D. Windisch, S. Hoffmann, S. Afonin, S. Vollmer, S. Benamira, B. Langer, J. Bürck, C. Muhle-Goll, A.S. Ulrich, Structural role of the conserved cysteines in the dimerization of the viral transmembrane oncoprotein E5, Biophys. J. 99 (2010) 1764–1772.
[84] M.J. Klein, S.L. Grage, C. Muhle-Goll, J. Bürck, S. Afonin, A.S. Ulrich, Structure analysis of the membrane-bound PhoD signal peptide of the Tat translocase shows an N-terminal amphiphilic helix, Biochim. Biophys. Acta 1818 (2012) 3025–3031.
[85] M. Paulmann, T. Arnold, D. Linke, S. Özdirekcan, A. Kopp, T. Gutsmann, H. Kalbacher, I. Wanke, V.J. Schuenemann, M. Habeck, J. Bürck, A.S. Ulrich, B. Schittek, Structure-activity analysis of the dermcidin-derived peptide DCD-1 L, an anionic antimicrobial peptide present in human sweat, J. Biol. Chem. 287 (2012) 8434–8443.
[86] T. Steinbrecher, S. Prock, J. Reichert, P. Wadhwani, B. Zimpfer, J. Bürck, M. Berditsch, M. Elstner, A.S. Ulrich, Peptide-lipid interactions of the stress-response peptide TisB that induces bacterial persistence, Biophys. J. 103 (2012) 1460–1469.
[87] G.B. Fields, R.L. Noble, Solid-phase peptide synthesis utilizing 9-fluorenylmethoxycarbonyl amino acids, Int. J. Pept. Protein Res. 35 (1990) 161–214.
[88] C.N. Pace, F. Vajdos, L. Fee, G. Grimsley, T. Gray, How to measure and predict the molar absorption coefficient of a protein, Protein Sci. 4 (1995) 2411–2423.
[89] W.C. Johnson, Analyzing protein circular dichroism spectra for accurate secondary structures, Proteins 35 (1999) 307–312.
[90] N. Sreerama, S.Y. Venyaminov, R.W. Woody, Estimation of protein secondary structure from circular dichroism spectra: inclusion of denatured proteins with native proteins in the analysis, Anal. Biochem. 287 (2000) 243–251.
[91] S.W. Provencher, J. Glockner, Estimation of globular protein secondary structure from circular dichroism, Biochemistry 20 (1981) 33–37.
[92] I.H. van Stokkum, H.J. Spoelder, M. Bloemendal, R. van Grondelle, F.C. Groen, Estimation of protein secondary structure and error analysis from circular dichroism spectra, Anal. Biochem. 191 (1990) 110–118.
[93] N. Sreerama, S.Y. Venyaminov, R.W. Woody, Estimation of the number of α-helical and β-strand segments in proteins using circular dichroism spectroscopy, Protein Sci. 8 (1999) 370–380.
[94] N. Sreerama, R.W. Woody, A self-consistent method for the analysis of protein secondary structure from circular dichroism, Anal. Biochem. 209 (1993) 32–44.
[95] L. Whitmore, B.A. Wallace, DICHROWEB, an online server for protein secondary structure analyses from circular dichroism spectroscopic data, Nucleic Acids Res. 32 (2004) W668–W673.
[96] A. Lobley, L. Whitmore, B.A. Wallace, DICHROWEB: an interactive website for the analysis of protein secondary structure from circular dichroism spectra, Bioinformatics 18 (2002) 211–212.
[97] M. Rance, R.A. Byrd, Obtaining high-fidelity spin-1/2 powder spectra in anisotropic media - phase-cycled Hahn echo spectroscopy, J. Magn. Reson. 52 (1983) 221–240.
[98] B.M. Fung, A.K. Khitrin, K. Ermolaev, An improved broadband decoupling sequence for liquid crystals and solids, J. Magn. Reson. 142 (2000) 97–101.
[99] S. Zhang, X.L. Wu, M. Mehring, Elimination of ringing effects in multiple-pulse sequences, Chem. Phys. Lett. 173 (1990) 481–484.
[100] A.E. Bennett, C.M. Rienstra, M. Auger, K.V. Lakshmi, R.G. Griffin, Heteronuclear decoupling in rotating solids, J. Chem. Phys. 103 (1995) 6951–6958.
[101] M.H. Levitt, D. Suter, R.R. Ernst, Spin dynamics and thermodynamics in solid-state NMR cross polarization, J. Chem. Phys. 84 (1986) 4243–4255.
[102] C. Ammann, P. Meier, A.E. Merbach, A simple multi-nuclear NMR thermometer, J. Magn. Reson. 46 (1982) 319–321.
[103] G.A. Olah, H.W. Huang, Circular dichroism of oriented α-helices. 2. Electric field oriented polypeptides, J. Chem. Phys. 89 (1988) 6956–6962.
[104] E. Strandberg, P. Tremouilhac, P. Wadhwani, A.S. Ulrich, Synergistic transmembrane insertion of the heterodimeric PGLa/magainin 2 complex studied by solid-state NMR, Biochim. Biophys. Acta 1788 (2009) 1667–1679.
[105] P. Tremouilhac, E. Strandberg, P. Wadhwani, A.S. Ulrich, Conditions affecting the re-alignment of the antimicrobial peptide PGLa in membranes as monitored by solid state ^{2}H-NMR, Biochim. Biophys. Acta 1758 (2006) 1330–1342.
[106] S. Özdirekcan, D.T.S. Rijkers, R.M.J. Liskamp, J.A. Killian, Influence of flanking residues on tilt and rotation angles of transmembrane peptides in lipid bilayers. A solid-state ^{2}H NMR study, Biochemistry 44 (2005) 1004–1012.
[107] E. Strandberg, S. Morein, D.T.S. Rijkers, R.M.J. Liskamp, P.C.A. Van der Wel, J.A. Killian, Lipid dependence of membrane anchoring properties and snorkeling behavior of aromatic and charged residues in transmembrane peptides, Biochemistry 41 (2002) 7190–7198.
[108] A.E. Daily, D.V. Greathouse, P.C.A. Van der Wel, R.E. Koeppe II, Helical distortion in tryptophan- and lysine-anchored membrane-spanning α-helices as a function of hydrophobic mismatch: a solid-state deuterium NMR investigation using the geometric analysis of labeled alanines method, Biophys. J. 94 (2008) 480–491.
[109] P. Tremouilhac, E. Strandberg, P. Wadhwani, A.S. Ulrich, Synergistic transmembrane alignment of the antimicrobial heterodimer PGLa/magainin, J. Biol. Chem. 281 (2006) 32089–32094.
[110] A. Giangaspero, L. Sandri, A. Tossi, Amphipathic α helical antimicrobial peptides, Eur. J. Biochem. 268 (2001) 5589–5600.
[111] N.J. Gleason, V.V. Vostrikov, D.V. Greathouse, C.V. Grant, S.J. Opella, R.E. Koeppe II, Tyrosine replacing tryptophan as an anchor in GWALP peptides, Biochemistry 51 (2012) 2044–2053.